0888-8809/07/$15.00/0
Printed in U.S.A.

Molecular Endocrinology 21(11):2785–2794

doi: 10.1210/me.2007-0167

Overexpression of Micro Ribonucleic Acid 29, Highly Up-Regulated in Diabetic Rats, Leads to Insulin Resistance in 3T3-L1 Adipocytes

Aibin He, Liuluan Zhu, Nishith Gupta, Yongsheng Chang, and Fude Fang

The National Laboratory of Medical Molecular Biology (A.H., L.Z., Y.C., F.F.), Institute of Basic Medical Sciences, The Chinese Academy of Medical Sciences and Peking Union Medical College, Beijing 100005, China; and Department of Molecular Parasitology (N.G.), Humboldt University, Berlin 10115, Germany

Micro-RNAs (miRNAs) have been suggested to play pivotal roles in multifarious diseases associated with the posttranscriptional regulation of protein-coding genes. In this study, we aimed to investigate the function of miRNAs in type 2 diabetes mellitus. The miRNAs expression profiles were examined by miRNA microarray analysis of skeletal muscles from healthy and Goto-Kakizaki rats. We identified four up-regulated miRNAs, and 11 miRNAs that were down-regulated relative to normal individuals. Among induced miRNAs were three paralogs of miR-29, miR-29a, miR-29b, and miR-29c. Northern blotting further confirmed their elevated expression in three important target tissues of insulin action: muscle, fat, and liver of diabetic rats. Adenovirus-mediated overexpression of miR-29a/b/c in 3T3-L1 adipocytes could largely repress insulin-stimulated glucose uptake, presumably through inhibiting Akt activation. The increase in miR-29 level caused insulin resistance, similar to that of incubation with high glucose and insulin in combination, which, in turn, induced miR-29a and miR-29b expression. In this paper, we demonstrate that Akt is not the direct target gene of miR-29 and that the negative effects of miR-29 on insulin signaling might be mediated by other unknown intermediates. Taken together, these data reveal the crucial role of miR-29 in type 2 diabetes. (*Molecular Endocrinology* 21: 2785–2794, 2007)

MICRO-RNAs (miRNAs) are a class of noncoding, 21- to 23-nucleotides long RNA. They serve as the important posttranscriptional regulators that down-regulate the expression of their target genes. They inhibit protein translation or induce mRNA degradation, depending on the partial or complete seed match to their target sites (1). In mammals, miRNAs have been implicated in modulation of temporal development (2, 3), adipocyte and myoblast differentiation (4, 5), and hematopoiesis (6). In addition, miRNAs have also been associated with cancer, neurological disorders, and other developmental diseases (7–11).

Type 2 diabetes mellitus (T2DM) is a complex, multisystemic disease with a pathophysiology that includes hyperinsulinemia and hyperglycemia along with other metabolic impairments (12, 13). Many studies have attempted to uncover the expression profiles of coding gene in muscle, fat tissue, and liver of T2DM-suffering individuals. More recently, elegant investigations have provided the evidence that miRNAs may regulate mammalian metabolic processes linked to T2DM including insulin signaling. The study by Poy *et al.* (15) suggested the involvement of miRNAs in yet another specialized cell function, insulin exocytosis, in which the pancreatic islet-specific miRNA, mir-375, plays a negative role in insulin secretion by these cells. This miRNA is also a key determinant of blood glucose homeostasis, indicating the participation of miRNAs in T2DM (14, 15). Additionally, the adipocyte differentiation and function can be regulated by miRNAs: miR-143 promotes adipogenesis by an unknown mechanism; let-7c increases peroxisome proliferator-activated receptor-γ2 (a key regulator of adipocyte function) expression in adipocytes; and six additional miRNAs alter the markers of adipocyte differentiation (2). Further, miRNA-122 has been shown to directly regulate lipid metabolism *in vivo*: administration of miR-122 antisense oligonucleotides to mice increases fatty acid oxidation in liver and decreases fatty acid synthesis (16). Finally, the members of miR-1 family, miR-133 and miR-181, are involved in myogenesis and myoblast differentiation, respectively (17, 18).

The objective of this work is to explore the differential spectrum of miRNA under type 2 diabetic and normal states and to investigate specific miRNAs implicated in

First Published Online July 24, 2007

Abbreviations: Ad-eGFP, Adenovirus comprising enhanced green fluorescent protein; FBS, fetal bovine serum; GLUT, glucose transporter; GK, Goto-Kakizaki; IR, insulin receptor; IRS, insulin receptor substrate; KRH, Krebs-Ringer-HEPES; LNA, locked nucleic acid; miR-29, micro-RNA 29; miRNA, micro-RNA; PI3K, phosphatidylinositol 3-kinase; SDS, sodium dodecyl sulfate; SREBP, sterol regulatory element-binding protein; SSC, standard sodium citrate; TCL1, T-cell leukemia 1; T2DM, type 2 diabetes mellitus.

***Molecular Endocrinology* is published monthly by The Endocrine Society (http://www.endo-society.org), the foremost professional society serving the endocrine community.**

T2DM. Microarray and Northern blot analyses were used to identify and validate the distinct expression of 15 miRNAs. Three paralogs of miR-29 family were up-regulated in all three major insulin-responsive organs of diabetic rats. These results prompted us to elucidate their function in insulin-signaling pathway and glucose homeostasis. Interestingly, mir-29a/b/c, upon their overexpression in 3T3-L1 adipocytes, repressed insulin-induced glucose uptake by cells. In addition, 3T3-L1 adipocytes treated with high levels of insulin plus glucose display up-regulation of their miR-29a and miR-29b populations in comparison with cells exposed to physiological concentration of glucose. These data suggest that the persistent exposure to high insulin and glucose might contribute to the increased expression of the miR-29 family. This study also demonstrates the indirect down-regulation of Akt activation by miR-29, which subsequently inhibits insulin-mediated glucose import by adipocytes.

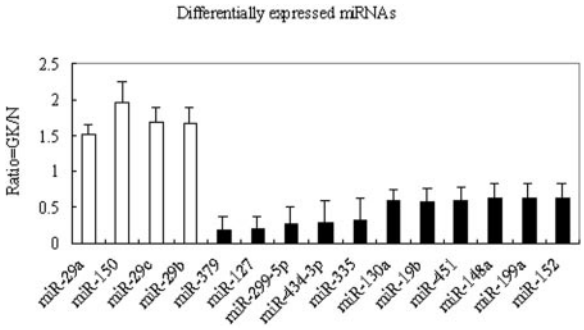

Fig. 1. Microarray Analysis Reveals the Differential Expression of miRNA in Skeletal Muscles of Diabetic Rats

The experiments were performed on two groups (GK diabetic rats and normal rats; two samples for each group). Probes were printed in triplicate on each chip, and the experiment was repeated twice. Raw data were normalized after subtraction using the global median of signal intensities. The normalized intensity ratio depicted in the figure is the fold change of GK/normal rats. Candidate miRNAs exhibiting the fold change of at least 1.5 were selected using quantitative Significance Analysis of Microarrays analysis. The up- and down-regulated miRNAs are indicated with *open and solid bars*, respectively. GK/N, GK/normal.

RESULTS

The miRNA Expression in the Diabetic Rat Is Distinctly Modulated

To investigate the potential involvement of miRNAs in T2DM, we performed the miRNA microarray analysis of the samples from normal Wistar and Goto-Kakizaki rats, which are established animal models for T2DM (see supplemental Table 1 published as supplemental data on The Endocrine Society's Journals Online web site at http://mend.endojournals.org). Microarray analysis (The microRNA Registry, Release 8.0) demonstrated that 15 miRNAs were differentially expressed in skeletal muscle tissue with the fold change of Goto-Kakizaki (GK)/control $\geq$1.5 (Fig. 1). Among four up-regulated miRNAs, we focused on three paralogs of miR-29 family that are highly expressed in diabetic rats: miR-29a, miR-29b, and miR-29c, all having the same seed sequence (Fig. 2A). A schematic sketch of their genomic loci is depicted in Fig. 2B: miR-29b2 and miR-29c are located on chromosome 13 and miR-29b1 and miR-29a are located on chromosome 4 in rats. Neither Hwang *et al.* (19) nor our group were able to annotate any promoter region in interval sequences of 29b1–29a and 29b2–29c clusters, suggesting that two distinct transcripts may be transcribed for these miRNAs. As anticipated, Northern blot analysis validated the increase in their expression in all three insulin-sensitive organs of diabetic rats, *i.e*. the skeletal muscle, liver, and fat tissues (Fig. 2, C and D).

High Glucose and Insulin Can Mimic the Insulin Resistance and Up-Regulate the Transcription of miR-29a and miR-29b, But Not of miR-29c, in 3T3-L1 Adipocytes

T2DM is characterized by hyperglycemia, hyperlipidemia, and the impairment of insulin action in peripheral tissues. Preincubation with high glucose and insulin in combination has been employed as a method to mimic *in vitro* insulin resistance in 3T3-L1 adipocytes (20, 21). During 3T3-L1 cell differentiation, the level of miR-29a-c transcripts diminished from d 1 to d 3 and increased subsequently (d 9, Fig. 3A). Since that time, cells were cultured in medium inclusive of three hormones: dexamethasone, iso-butylmethylxanthine, and insulin from d 1 to d 3, and in only insulin-supplemented medium from d 4 to d 6, the induction of miR-29 may have been caused by insulin. Therefore, we attempted to determine the relationship between miR-29 and insulin resistance. Upon preincubation of 3T3-L1 adipocytes with high glucose and insulin for 24 h, the expression of miR-29a and miR-29b was increased significantly (29a, 2.59 $\pm$ 0.09; 29b, 1.84 $\pm$ 0.06; $P < 0.005$) when compared with cells cultured at physiological concentrations of glucose in the absence of insulin (Fig. 3, B and C). However, we did not observe this incremental effect on miR-29c expression. Because the high level of insulin and glucose are regularly detected in insulin-responsive tissues of T2DM individuals, we assumed that miR-29a and miR-29b were up-regulated specifically by high glucose and insulin. Because the expression of miR-29c was not induced, it is also suggested that hyperglycemia and hyperinsulinemia may not be the only determinant factor for the induction of miR-29 in diabetic rats.

Overexpression of miR-29 Inhibits Insulin-Induced Glucose Import by 3T3-L1 Adipocytes

The expression patterns of miR-29a/b/c were similar in all insulin-sensitive tissues; hence, we investigated the

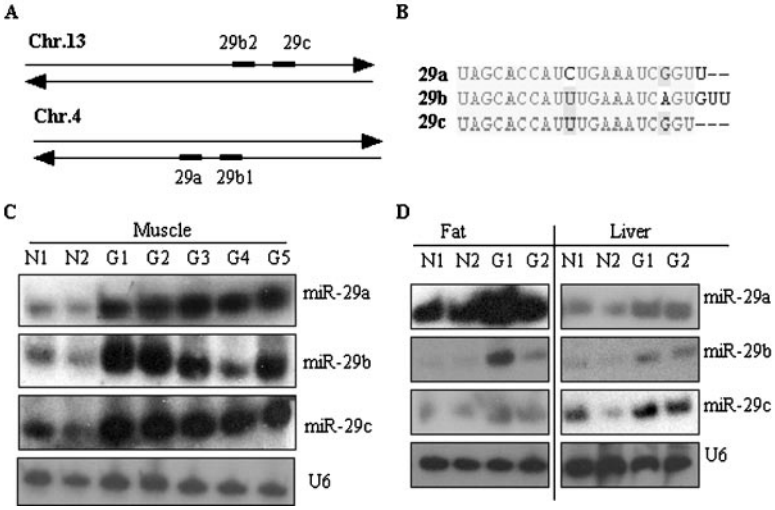

Fig. 2. Expression of miR-29 Paralogs in Rat Skeletal Muscles, Fat and Liver Tissues, and Their Loci on Chromosomes

Total RNA (30 μg) from each sample was used for the Northern blot analysis. To minimize the cross-reaction, each blot was probed for miR-29 and then reprobed with U6 small nuclear RNA for normalization. A, miR-29b-2/miR-29c and miR-29b-1/miR-29a clusters are shown on rat chromosome 13 and 4, respectively. B, Sequences of all three miR-29 paralogs. C, Two skeletal muscle samples from normal and five samples from diabetic rats were analyzed. D, Two samples from each, fat or liver, for all groups were used. Chr., Chromosome; N, normal rat; G, Goto-Kakizaki rat.

influence of the miR-29 family on glucose homeostasis regulated by insulin and on insulin-signaling pathway. As shown in Fig. 2A, these miRNAs are highly conserved and have identical nucleotides from second to seventh base known as the "seed" sequence. It is considered to be the most critical sequence for selecting targets. These miRNAs, therefore, may have overlapping target genes regulated at their posttranscriptional level. To address their functional relevance in cellular signaling, we coexpressed three miRNAs of miR-29 family in 3T3-L1 adipocytes. This cell line serves as an excellent model to study the insulin-signaling pathway. To achieve efficient transfection of 3T3-L1 cells, we generated a recombinant adenovirus (Ad-29) coexpressing miR-29a, miR-29b, and miR-29c in a single transcript, and a control adenovirus comprising enhanced green fluorescent protein (Ad-eGFP). Northern blot analysis illustrated that 3T3-L1 infected with Ad-29 (multiplicity of infection = 2000) enabled a 4- to 6-fold increase in the levels of mature miR-29a, miR-29b, and miR-29c expression, although both their endogenous and ectopic precursors were undetectable (Fig. 4A).

To elucidate the effect of elevated miR-29 on insulin resistance in diabetic rats, we measured insulin-induced glucose uptake in adenovirus-infected 3T3-L1 adipocytes. Glucose import was reduced to approximately 50% ($P = 0.001$) in 3T3-L1 infected with Ad-29 in comparison with Ad-eGFP. In contrast, miR-29 did not affect glucose uptake in the basal state of adipocytes (Fig. 4B), which suggested that miR-29 might function by silencing component(s) of insulin-signaling pathways. These interesting findings prompted us to test whether the inhibition of miR-29 function might reverse this phenomenon of insulin-modulated glucose uptake. Cells were transfected with inhibitor of miR-29, the antisense oligonucleotides locked nucleic acid (LNA), and assayed for glucose uptake 2 d after transfection. No significant-change in glucose uptake (Mock/ins, 4.30 $\pm$ 0.38; inhibitor/ins, 5.07 $\pm$ 0.23; $P = 0.16$) was observed in cells treated with insulin (Fig. 4C), which could be ascribed to the relatively low endogenous expression of miR-29 as shown in Fig. 3A. These data implicate a negative regulatory role of miR-29 in insulin-signaling pathways.

miR-29 Can Modulate Intracellular Insulin Signaling by Down-Regulating Akt Activation

Because insulin-dependent glucose import could be compromised by the overexpression of miR-29 in 3T3-L1 adipocytes; it was crucial to examine whether insulin-signaling pathway was dampened. Two upstream signals in insulin-initiated cascade are the expression of insulin receptor (IR) and IR substrate-1 (IRS-1) proteins. As depicted in Fig. 5A, total cellular content of IR and IRS-1 was unchanged in Ad-29-infected cells. The level of IR phosphorylation (Tyr 1162/1163) in miR-29-expressing adipocytes was also not significantly affected ($P = 0.15$). These data contradict two reports in which high glucose and insulin in primary rat adipocytes and L6 myotubes led to the reduction in IR and IRS-1 protein content and insulin-mediated tyrosine phosphorylation of IR (12, 22). However, our result is consistent with other studies revealing that high glucose plus insulin affect neither the pool of IR and IRS-1 proteins nor the tyrosine phosphorylation of IR, when compared with control cells treated with a physiological concentration of glucose (5 mM) (Fig. 5B) (20, 23). Surprisingly, the total tyrosine

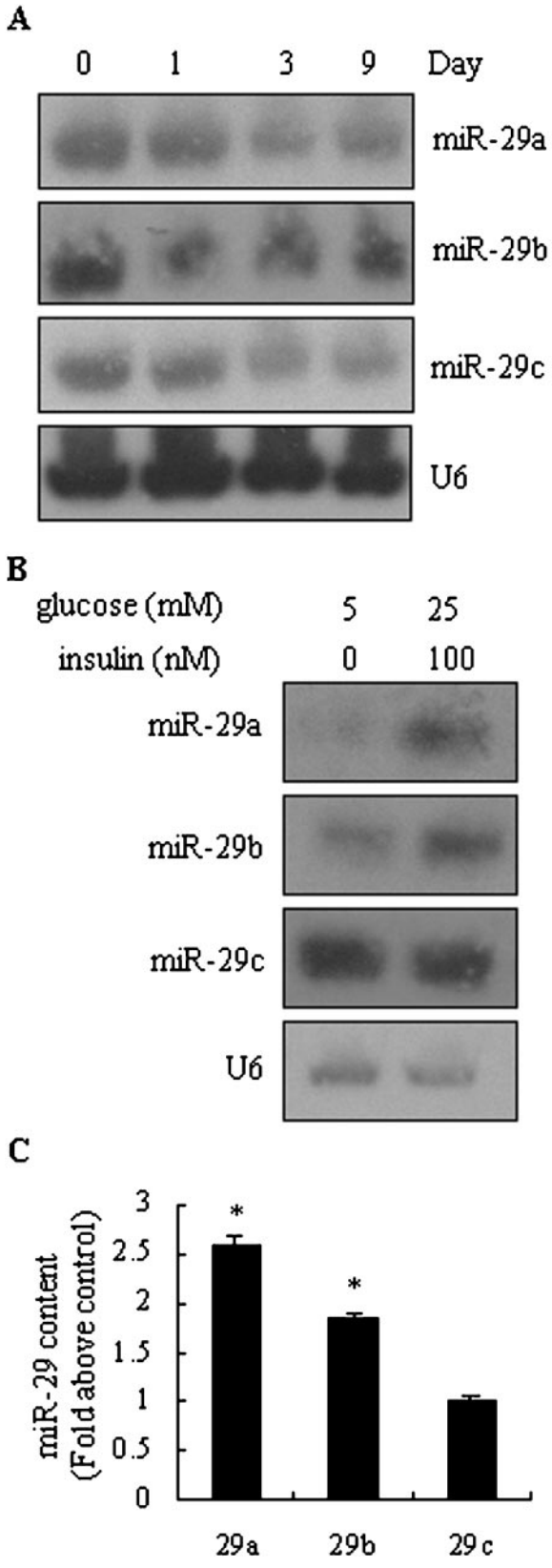

Fig. 3. The Expression of miR-29a and miR-29b, But Not of miR-29c, Is Up-Regulated by Insulin in 3T3-L1 Adipocytes

A, A time-course Northern blot of miR-29a, miR-29b, and miR-29c expressed during 3T3-L1 differentiation. Total RNA (30 μg) was used for each sample. B, After the induced differentiation (9 d) of 3T3-L1 preadipocytes into adipocytes, one group was treated with 5 mM glucose (control) and the other with 25 mM glucose and 100 nM insulin (high glc&ins; 24 h, 37 C, 5% CO_2). Total RNA (30 μg) from differentiated 3T3-L1 cells was loaded in each lane for Northern analysis. The depicted blot is representative of three independent experiments. C, Densitometry data were obtained using Genetools software and expressed as the ratio change in miR-29a-c for high glc&ins/control samples. *, $P < 0.05$.

phosphorylation of IRS-1 was modestly but reproducibly decreased by 21% ($P = 0.023$) in Ad-29-infected cells compared with control cells (Fig. 5, C and E). Furthermore, as shown in Fig. 5C, insulin also repressed IRS-1-associated p85, the regulatory subunit of phosphatidylinositol 3-kinase (PI3K), by 37% ($P = 0.003$). We also found that high Glc/insulin pretreatment led to insulin-insensitive reaction as indicated by no insulin-inducible increase in phosphorylated IRS-1 and IRS-1-associated p85 (Fig. 5D). Thus, it is concluded that the presence of high glucose and insulin or the overexpression of miR-29 can modulate proximal signals of insulin-initiated cascade.

We also examined the key distal molecules in the insulin-signaling pathway. Akt, a protein downstream to PI3K, is required for glucose transporter (GLUT)4 translocation to cell surface upon stimulation with insulin, subsequently augmenting the glucose transport (24, 25). Upon insulin treatment of adipocytes overexpressing miR-29, Akt phosphorylation was attenuated by 59% ($P = 0.001$, Fig. 5, B and E). Our data are in accordance with a report that high glucose and insulin can inhibit the phosphorylation of Akt at Ser 473, which must be activated for downstream signaling (22). Taken together, these data implicate the concomitant impairment of cellular Akt activation and desensitization to glucose transport in 3T3-L1 adipocytes.

The Inhibition of miR-29 Can Potentiate Insulin-Stimulated Akt Phosphorylation

As demonstrated, Ad-miR-29 has the potential to inhibit Akt activation and subsequently block insulin-induced glucose uptake in 3T3-L1 adipocytes. We questioned whether the inhibition of miR-29 function would reverse its effect on insulin-mediated Akt activation and glucose uptake. To address this issue, we designed an LNA antisense-based loss-of-function assay. LNA-antisense oligonucleotides can form highly stable sequence-specific duplexes with their corresponding target miRNAs and potently attenuate these molecules (18). Using an oligonucleotide complementary to one of miR-29a/b/c, miR-29 inhibition was evident at the functional level, which was assayed by means of luciferase reporter construct harboring a sequence complementary to miR-29b (data not shown). As expected, LNA antisense inhibition of miR-29 in 3T3-L1 cells improved Akt activation in the

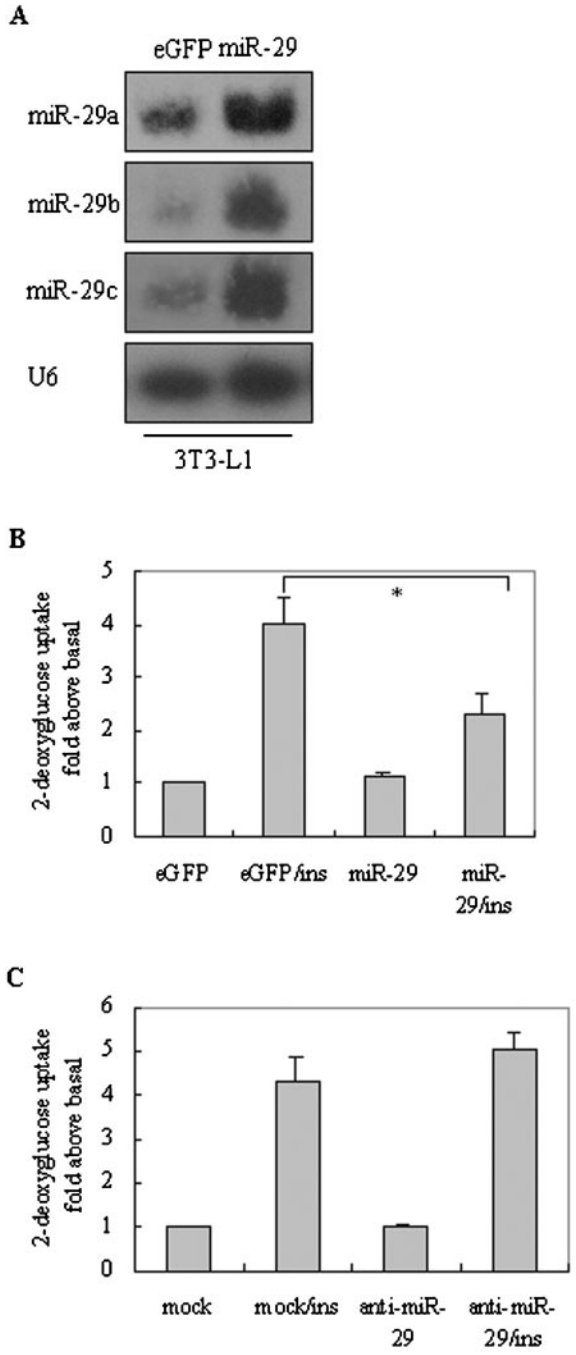

Fig. 4. Adenovirus-Mediated Overexpression of miR-29 Leads to Impaired Glucose Uptake in Response to Insulin

A, The DNA construct inclusive of three miR-29 paralogs was expressed in recombinant adenovirus (Ad-miR-29), and adenovirus with eGFP was used as control (Ad-eGFP). On d 5–6 of differentiation, 3T3-L1 cells were infected with Ad-GFP or Ad-miR-29 as described in *Materials and Methods*. Northern blot analysis of cells at 3 d after infection was performed. B, [^{3}H]2-deoxyglucose uptake by cells infected with Ad-eGFP or Ad-miR-29. The value of 1 was assigned to the basal condition in which cells were infected with Ad-eGFP. C, [^{3}H]2-deoxyglucose uptake by cells transfected with anti-ath-miR156a antisense LNA (300 nM) (control) or anti-miR-29a-c antisense LNA (100 nM for each miR-29 paralog). The data are expressed as the mean values ± SEM. *, $P < 0.05$ between two groups (n = 3–5, each condition). Ins, Insulin.

presence of insulin at 37 C. The extent of Akt phosphorylation was more profound at 5 min than at 15 min incubation with insulin (5 min, 2.75 ± 0.10, $P = 0.0001$; 15 min, 1.32 ± 0.09, $P = 0.02$) (Fig. 6, A and B). In contrast, the silencing of miR-29 did not change the basal Akt activation, because its phosphorylation was undetectable in the absence of insulin. Then, we also examined, whether the blockade of endogenous miR-29 would allow improvement in glucose transport in response to insulin. In fact, LNA inhibition of miR-29 barely augmented insulin-dependent glucose uptake (Fig. 4C), reflecting considerable discrepancy between enhanced Akt activation and improved glucose uptake. This result might be due to the involvement of numerous other target molecules of insulin-signaling pathway. Whether this difference is due to distinct bias of miR-29 on its target genes requires further investigation. Collectively, our data implicate a therapeutic function of miR-29 during diabetes, wherein its expression is higher than the normal condition.

DISCUSSION

Recently, the understanding of miRNA-regulatory networks governing cell physiology and diseases has rapidly evolved. The pancreatic islet-specific miR-375, for the first time, was found to regulate insulin secretion and may play an important role in T2DM (15). In this study, we have identified the differential expression pattern of miRNAs in diabetic GK and normal rats. Our work focused on three miRNAs of four up-regulated miRNAs in GK rat because they belong to the miR-29 family and exhibit similar expression profiles in all three insulin-responsive tissues. These data strongly implicated their involvement in the insulin-signaling cascade. Insulin resistance is an important characteristic of T2DM, and hyperglycemia along with hyperinsulinemia can contribute to its further deterioration (22). This research demonstrates that hyperinsulinemia together with hyperglycemia conferred an increase in expression of miR-29a and miR-29b, but not of miR-29c (for unknown reasons). Presumably, miR-29b is transcribed in two independent transcripts (Fig. 2A), which might contribute to higher miR-29b expression than that of miR-29a and miR-29c. These data also indicate that two clusters might be subjected to independent regulation at their transcriptional level, because only one cluster of miR-29b1-miR-29a was modulated by hyperinsulinemia and hyperglycemia. Although the higher amount of miR-29 family transcripts at the cellular and the whole-body level already existed, hyperinsulinemia and hyperglycemia contributed further to their elevated expression. The overexpression of miR-29 into 3T3-L1 adipocytes confers insulin resistance as demonstrated by the impairment of insulin-stimulated glucose uptake. Therefore, based on these data, we propose that high insulin promotes an increase in miR-29 transcripts, which consequently

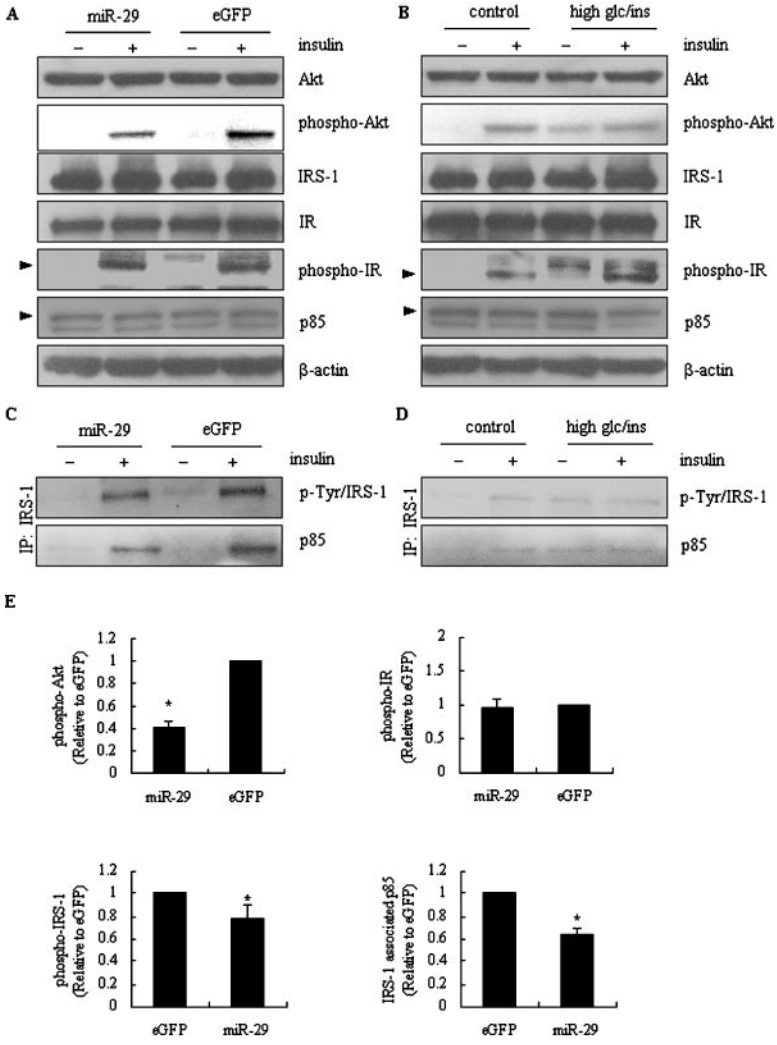

Fig. 5. Akt Phosphorylation Is Impaired in Ad-miR-29-Infected 3T3-L1 Adipocytes as Well as in Cells Exposed to High Glucose and Insulin

A, 3T3-L1 adipocytes infected with Ad-eGFP or Ad-miR-29 were stimulated with 100 nM insulin for 15 min, or left untreated. B, 3T3-L1 adipocytes were incubated in 5 mM glucose alone or 25 mM glucose and 200 nM insulin for 24 h. A and B, 60 μg of protein from total cellular lysate was separated on SDS-PAGE, followed by immunoblotting with anti-Akt, anti-phosphorylated Akt (Ser 473), anti-IRS-1, anti-IRβ, antiphosphorylated-IR (Tyr 1162/1163), anti-p85α, and anti-β-actin antibodies. The blots shown here are representative of at least three independent experiments. C and D, IRS-1 was immunoprecipitated from 500 μg of total cell lysate and immunoblotted for phosphorylated IRS-1 with antibody against phosphorylated tyrosine, and for IRS-1-associated p85 using anti-p85 antibody. The panels represent three individual experiments. E, Densitometry data were obtained using Genetools software and expressed as the *bar graph* of phosphorylated-Akt (473), phosphorylated-IR (Tyr 1162/1163), Tyr-phosphorylated-IRS-1, and IRS-1-associated p85 in insulin-stimulated and Ad-eGFP- or Ad-miR-29-infected cells. An arbitrary unit of 1 was assigned to insulin-stimulated eGFP sample. *, $P < 0.05$. glc/ins, Glucose/insulin; IP, immunoprecipitation.

inhibit the insulin-signaling pathway through a negative feedback control.

Additionally, the ectopic expression of miR-29 caused the decline in glucose transport induced by insulin; therefore, we investigated the target proteins of miR-29. Potential candidate genes were examined by luciferase reporter system and/or Western blotting analysis. From hundreds of predicted target genes of miR-29a/b/c, two candidates including INSIG1 and CAV2 were confirmed by luciferase reporter system analysis and immunoblotting (supplemental Fig. S1 published as supplemental data on The Endocrine Society's Journals Online web site at http://mend.endojournals.org) (26–29). Insig1 is a significant integrator of nutrient and hormonal signals that can be induced by insulin and regulates the sterol regulatory element-binding protein/adipocyte determination and differentiation factor 1 (SREBP/ADD1) cleavage and formation of its nuclear isoform (30–32). In addition, our data along with others (33) reveal that the expression of cav2 in skeletal muscle and liver tissue of diabetic rats is decreased significantly in relation to the

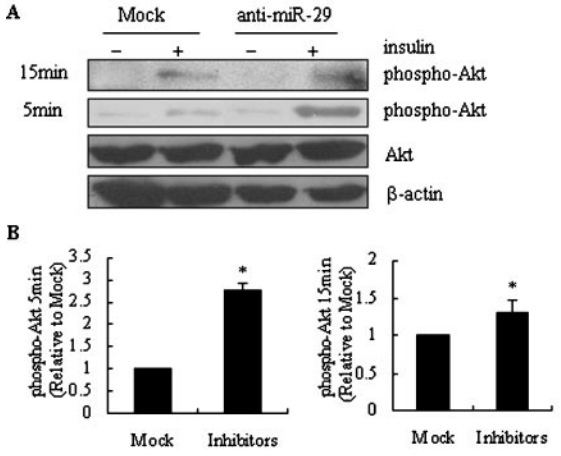

Fig. 6. Anti-miR-29 Antisense LNA Oligonucleotides Augment Insulin-Mediated Akt Phosphorylation

A, 3T3-L1 adipocytes were transfected with 200 nmol/liter of anti-ath-miR156a antisense LNA (mock) or a mixture of anti-miR-29 antisense LNA by means of siPORT NeoFX agent. Cells were subjected to immunoblotting 48 h after transfection using anti-Akt, anti-phosphorylated Akt, and anti-β-actin antibodies. Insulin treatment was for 5 or 15 min. Representative data of three experiments are depicted. B, Densitometry data were obtained using Genetools software and expressed as the *bar graph* of phosphorylated-Akt (Ser-473) in cells treated with insulin for 5 or 15 min. An arbitrary unit of 1 was assigned to insulin-treated mock condition. *, $P < 0.05$.

healthy control group. However, this reduction in cav2 was not visible in fat tissue, as indicated by Western blotting analysis (supplemental Fig. S1C). In diabetic tissues, they are reflected as higher level of miR-29 and the decreased expression of cav2 (Fig. 1 and supplemental Fig. S1C) vindicating cav2 as a *bona fide* target of miR-29. In fact, the overexpression of miR-29 inhibited cav2 protein expression as verified by Western blotting (supplemental Fig. S1B). Finally, in IR-overexpressed rat fibroblast cells, insulin induces cav2 expression and influences the downstream cascade (34). Cav2 is not known to participate directly in the insulin-signaling pathway, and further *in vivo* studies are needed to test whether or not higher levels of miR-29 would contribute to the down-regulation of cav2 expression. Collectively, these data confirm the functional association of cav2 with T2DM. In addition, syntaxin-1, a participant in GLUT4 vesicle fusion to the plasma membrane via its interaction with munc18, has been predicted to be a target of miR-29 (35, 36). Syntaxin-1 is also required for rapid exocytosis of insulin in pancreatic β-cells (37), and high glucose and lipid result in disappearance of syntaxin-1 in T2DM (38). These data suggest that syntaxin-1 may be another noteworthy target in T2DM.

To establish the relationship between the abnormal expression of miR-29 and inflicted diabetic malfunctions at the biochemical and physiological level, we examined multiple key regulators of the insulin-signaling pathway. Insulin, upon binding to its receptor (IR), activates its intrinsic protein tyrosine kinase activity resulting in initiation of a cascade of key downstream molecules including IRS-1, IRS-2, PI3K, phosphoinositide-dependent protein kinase 1, Akt, and PKCζ/λ. This signaling eventually leads to an insulin-stimulated GLUT4 translocation to the cell surface and its subsequent activation (39). Similar to the insulin resistance caused by preincubation with high glucose and insulin for 24 h, the introduction of miR-29 into adipocytes did not affect the upstream signaling events, such as the content of IR and IRS-1 and the tyrosine phosphorylation of IR. However, the activation of Akt by insulin, as determined by the phosphorylation of Akt at 473-Ser, was significantly inhibited. Total tyrosine phosphorylation of IRS-1 and the expression of IRS-1-associated p85 were also diminished. The silencing of endogenous miR-29a/b/c exerted a positive impact on insulin-stimulated Akt activation. Moreover, increasing evidence suggests Akt to be an important regulator of Glut4 translocation and glucose import (24). Taken together, it can be postulated that the events of insulin signaling leading to glucose uptake involve the reduction in IRS-1-associated p85 content and impairment of Akt activation by elevated miR-29. The mechanism of miRNA action on Akt activation is still unclear. Pekarsky *et al.* (40) have identified and validated TCL1 (T-cell leukemia 1) as a target of miR-29 in B cells. The protooncogene TCL1 has been shown to interact with the Akt pleckstrin homology domain and enhance Akt kinase activity. Hence, it may function as a coactivator of Akt kinase (41). The indirect repression of Akt activation through the down-regulation of TCL1 by miRNAs would be a potential mechanism explaining the association between the latter and T2DM. Further studies are needed to address this question.

Previous reports suggest the role of miRNAs as fine-tuning devices rather than being the primary gene regulators (42, 43). Nonetheless, the collective modulatory influence of a single miRNA on hundreds of its target genes might exert a considerable change in cell physiology and progression of diseases (44). Our data demonstrate that many insulin-initiated signals are down-regulated by ectopic overexpression of miR-29. Two key insulin-responsive proteins, insig1 and cav2, were profoundly decreased by miR-29. Moreover, Akt activation, one of the most important steps in insulin-signaling pathways, was diminished, although no apparent effect on its cellular expression was evident. The major effect of miRNA on insulin-regulated glucose homeostasis further supports our assumption. Meanwhile, we also observed that the expression of SREBP and its cleaved-mature form, SREBP1c, were decreased in Ad-miR-29-infected 3T3-L1 cells (data not shown). In addition to the posttranscriptional control of insig1 expression through miR-29, the reduction in mature srebp1c may also contribute to the decline in insig1. More interestingly, the expression and cleavage of srebp1c is also induced by insulin; hence,

srebp1c may be another potential miR-29-regulated molecule. In conclusion, this study defines a model to explore the function of miR-29 in insulin-initiated cell signaling and consolidates the crucial role of miRNAs as the ribo-regulator of glucose homeostasis in T2DM.

MATERIALS AND METHODS

Animals, Cells, and Reagents

Cell culture reagents were purchased from Life Technologies, Inc. (Gaithersburg, MD), and other chemicals were from Sigma Chemical Co. (St. Louis, MO) unless specified otherwise. Anti-IRβ (sc-711), antiphosphorylated IRβ (Tyr 1162/1163) (sc-25103-R), anti-IRS-1 (sc-559), anti-p85α (PI3K) (sc-1637), antiphosphotyrosine (sc-7020), and anti-Insig1 (sc-25124) antibodies were obtained from Santa Cruz Biotechnology, Inc. (Santa Cruz, CA). Monoclonal antibody against caveolin-2 (mAb 65) was purchased from Transduction Laboratories, Inc. (Lexington, KY) and anti-β-actin antibody was purchased from Sigma. Monoclonal antibody against SREBP1 was purified from cell culture supernatants of hybridomas 2A4 (American Type Culture Collection, Manassas, VA). The enhanced chemiluminescence detection kit was from Amersham Pharmacia Biotech (Piscataway, NJ). LNA probes were constructed by Exiqon (Vedbaek, Denmark).

Male Wistar control and diabetic GK rats were obtained from SLACCAS (Shanghai, China). Both groups of rats were 2–3 months old and had similar body weights (250–300 g). Blood glucose levels in nonfasting rats were 5.1 $\pm$ 0.6 mM in the control (n = 5) and 13.5 $\pm$ 0.5 mM in the GK rats (n = 5). The rats were killed by decapitation after a brief exposure to carbon dioxide. Their skeletal muscles, sc fat tissue, and liver were collected and immediately frozen in liquid nitrogen for later use. All animal experiments had prior approval of "The Animal Care & Welfare Committee" of Peking Union Medical College.

293A cell lines were purchased from ATCC and incubated in α-MEM supplemented with 10% fetal bovine serum (FBS). 3T3-L1-mycGLUT4 cells were a kind gift of Dr. Konstantin V. Kandror and cultured in DMEM containing 10% FBS. Cells were grown until they became confluent and maintained for an additional 2 d. Differentiation was induced on d 0 by the addition of 0.5 mM methyl-isobutylxanthine (M), 0.5 μM dexamethasone (D), and 10 μg/ml insulin (I) in DMEM supplemented with 10% FBS (DMEM-MDI). On d 3, the DMEM-MDI medium was replaced with DMEM-10% FBS, which was replenished every 2 d. On d 7, more than 80% of cells had differentiated into adipocytes, which were then infected with adenovirus, or subcultured into six-well plates for glucose uptake assay. At least 90% cells displayed the standard phenotype of adipocytes before experimentation.

Microarray and Northern Blot Analyses of miRNA

Total RNA from tissues and cells was extracted using TRIzol RNA isolation kit (Invitrogen, Carlsbad, CA) according to the manufacturer's instructions. The miRNAs were purified from 50–100 μg of total RNA using the miRNA isolation kit (Ambion, Inc., Austin, TX). Purification of miRNA samples, labeling, and hybridization analysis were executed as described by the manufacturer. The data were extracted by SpotData-Pro software (CapitalBio, Beijing, China), and the differential miRNAs were selected using the program Significance Analysis of Microarrays (version 2.1). Nonredundant mature human, mouse, and rat miRNA sequences were downloaded from the miRNA registry (45). In total, 469 miRNA probes were designed that were complementary to the full-length mature miRNA. For Northern blot analysis, 10–30 μg of total RNA was separated on 15% denaturing polyacrylamide gels and electrotransferred to Hybond N^+ membrane (Amersham Biosciences, Little Chalfont, UK). The membranes were UV cross-linked with samples facing upward, prehybridized for 1 h, and then subjected to overnight hybridization with 5′-^{32}P-end-labeled oligonucleotide probes at 37 C. The membranes were rinsed twice with 1$\times$ standard sodium citrate (SSC) plus 0.1% sodium dodecyl sulfate (SDS) at room temperature, extensively washed in 0.5$\times$ SSC plus 0.1% SDS at 37 C, and then exposed to Kodak Biomax MS x-ray film at $-$80 C (Eastman Kodak, Rochester, NY). To strip off probes from the hybridized membranes for their reuse, they were incubated in 0.5% SDS at 100 C (5 min), washed in 2$\times$ SSC (5 min), and rehybridized as described above.

Western Blot Analysis

Proteins (50–100 μg) were fractionated by electrophoresis on 10% SDS polyacrylamide gel, electroblotted to polyvinylidene difluoride filter membranes for 2 h at 200 V. The polyvinylidene difluoride membranes were incubated with blocking buffer (50 mM Tris-HCl, pH 7.4; 150 mM NaCl; 0.1%Tween 20; 5% skimmed milk) for 1 h at room temperature, followed by overnight treatment with primary antibody at 4 C, and then with horseradish peroxidase-conjugated secondary antibody. After washing, the reactive bands were detected by enhanced chemiluminescence. Quantitative densitometry analysis of protein expression was performed using Genetools software (Syngene, Cambridge, UK).

Immunoprecipitation

IRS-1 was immunoprecipitated from total cell lysates as described previously (46, 47). Briefly, the whole-cell extracts were prepared by detergent solubilization in Nonidet P-40 lysis buffer (25 mM Tris-HCl, pH 7.4; 1% Nonidet P-40; 10% glycerol; 50 mM sodium fluoride; 10 mM sodium pyrophosphate; 137 mM sodium chloride; 1 mM sodium vanadate; 1 mM phenylmethylsulfonylfluoride, 10 μg/ml aprotinin, 1 μg/ml pepstatin, 5 μg/ml leupeptin) for 60 min at 4 C. Particulate material was separated from the soluble extract by microcentrifugation for 10 min at 4 C. The cell-free lysate (500 μg) was mixed with 4 μg of IRS-1 antibody and incubated overnight at 4 C followed by a second incubation with protein G-Sepharose for 4 h or overnight. The resultant immunoprecipitates were subjected to electrophoresis on 10% SDS-PAGE and subsequent immunoblotting with appropriate antibody.

[^{3}H]2-Deoxyglucose Uptake Assay

The experiment was performed in six-well plates. Cells were washed three times with 0.9% NaCl, serum-starved for 3 h followed by two washings with 37 C warm Krebs-Ringer-HEPES (KRH) buffer [121 mM NaCl, 4.9 mM KCl, 1.2 mM $MgS0_4$, 0.33 mM $CaCl_2$, 12 mM HEPES (pH 7.4)]. They were first treated with 100 nM insulin at 37 C for 15 min (optional) and then labeled with [^{3}H]2-deoxyglucose (0.1 mM, 0.625 μCi/ml) for 4 min (adipocytes or myotubes) or for 15 min (confluent preadipocytes or myoblast). The assay was terminated by removing the radioactive media followed by three washing steps with 1 ml of ice-cold KRH containing 25 mM D-glucose. Samples in each well were extracted with 200 μl of 0.1% SDS in glucose-free KRH buffer, and 150-μl aliquots were used to determine the cellular radioactivity by liquid scintillation counting. Under these conditions, glucose uptake was linear for at least 30 min. All measurements were made in duplicate and corrected for nonspecific diffusion as determined in the presence of 5 μM cytochalasin B, which

was below 10% of the total uptake. The protein concentration was estimated by BCA kit (Pierce Chemical Co., Rockford, IL), and used to normalize the counts as specific activity.

Construction of Recombinant Adenovirus

The recombinant adenovirus expressing miR-29a/b/c was generated by PCR. All miRNA precursor sequences were amplified using the following primers: the forward primer for 29b1–29a, 5′-CGAAGATCTGGATGAGGCCAGCATAGGAG-3′, the reverse primer for 29b1–29a, 5′-ATTTGCGGCCGC TCTTACCTGTGGCTCCAAAGTCA-3′; the forward primer for 29b2–29c, 5′-ATTTGCGGCCGCCATCTGCCTCTGTGATT-CTCAGG-3′, the reverse primer for 29b2–29c, 5′-CGCTCTA-GATGTAGGAAATGACAGGCTGATGC-3′. The fragments were cloned into shuttle vector AdTrack-cytomegalovirus. Ad-eGFP was used as the control construct. Cells were infected at indicated multiplicity of infection of viral particles in DMEM supplemented with 0.5 μg/ml of polylysine. The infection medium was substituted for DMEM-10% FBS 2 h after infection, and cells were cultured for 48–72 h before experimentation.

Statistical Analysis

Differences between treatments and/or groups were analyzed using an unpaired Student's *t* test. Only data with a statistical significance of $P < 0.05$ were considered.

Acknowledgments

We thank Dr. Yuguang Shi for helpful discussions and review of this manuscript and Dr. Konstantin V. Kandror for providing 3T3-L1/mycGlut4 cells as well as his useful instructions on glucose uptake assay.

Received April 3, 2007. Accepted July 19, 2007.

Address all correspondence and requests for reprints to: Dr. Fude Fang and Dr. Yongsheng Chang, Institute of Basic Medical Sciences, The Chinese Academy of Medical Sciences and Peking Union Medical College, 5 Dong Dan San Tiao, Beijing 100005, China. E-mail: fangfd@vip.sina.com and changyongsheng@yahoo.com.

This work was supported by grants from the Major State Basic Research Development Program of China (973 Program 2004CB518602 and 2006CB503909) and the National Natural Science Foundation of China (30471930).

Disclosure Statement: The authors have nothing to disclose.

REFERENCES

1. Bartel DP 2004 MicroRNAs: genomics, biogenesis, mechanism, and function. Cell 116:281–297
2. Esau C, Kang X, Peralta E, Hanson E, Marcusson EG, Ravichandran LV, Sun Y, Koo S, Perera RJ, Jain R, Dean NM, Freier SM, Bennett CF, Lollo B, Griffey R 2004 MicroRNA-143 regulates adipocyte differentiation. J Biol Chem 279:52361–52365
3. Kajimoto K, Naraba H, Iwai N 2006 MicroRNA and 3T3-L1 pre-adipocyte differentiation. RNA 12:1626–1632
4. Rao PK, Kumar RM, Farkhondeh M, Baskerville S, Lodish HF 2006 Myogenic factors that regulate expression of muscle-specific microRNAs. Proc Natl Acad Sci USA 103:8721–8726
5. Nakajima N, Takahashi T, Kitamura R, Isodono K, Asada S, Ueyama T, Matsubara H, Oh H 2006 MicroRNA-1 facilitates skeletal myogenic differentiation without affecting osteoblastic and adipogenic differentiation. Biochem Biophys Res Commun 350:1006–1012
6. Ramkissoon SH, Mainwaring LA, Ogasawara Y, Keyvanfar K, McCoy Jr JP, Sloand EM, Kajigaya S, Young NS 2006 Hematopoietic-specific microRNA expression in human cells. Leuk Res 30:643–647
7. Chen CZ 2005 MicroRNAs as oncogenes and tumor suppressors. N Engl J Med 353:1768–1771
8. Gregory RI, Shiekhattar R 2005 MicroRNA biogenesis and cancer. Cancer Res 65:3509–3512
9. Esquela-Kerscher A, Slack FJ 2006 Oncomirs—microRNAs with a role in cancer. Nat Rev Cancer 6:259–269
10. Zhang B, Pan X, Cobb GP, Anderson TA 2007 microRNAs as oncogenes and tumor suppressors. Dev Biol 302:1–12
11. Hede K 2005 Studies define role of microRNA in cancer. J Natl Cancer Inst 97:1114–1115
12. Huang C, Somwar R, Patel N, Niu W, Torok D, Klip A 2002 Sustained exposure of L6 myotubes to high glucose and insulin decreases insulin-stimulated GLUT4 translocation but upregulates GLUT4 activity. Diabetes 51:2090–2098
13. Kahn CR 1986 Insulin resistance: a common feature of diabetes mellitus. N Engl J Med 315:252–254
14. Gauthier BR, Wollheim CB 2006 MicroRNAs: 'ribo-regulators' of glucose homeostasis. Nat Med 12:36–38
15. Poy MN, Eliasson L, Krutzfeldt J, Kuwajima S, Ma X, Macdonald PE, Pfeffer S, Tuschl T, Rajewsky N, Rorsman P, Stoffel M 2004 A pancreatic islet-specific microRNA regulates insulin secretion. Nature 432:226–230
16. Esau C, Davis S, Murray SF, Yu XX, Pandey SK, Pear M, Watts L, Booten SL, Graham M, McKay R, Subramaniam A, Propp S, Lollo BA, Freier S, Bennett CF, Bhanot S, Monia BP 2006 miR-122 regulation of lipid metabolism revealed by in vivo antisense targeting. Cell Metab 3:87–98
17. Chen JF, Mandel EM, Thomson JM, Wu Q, Callis TE, Hammond SM, Conlon FL, Wang DZ 2006 The role of microRNA-1 and microRNA-133 in skeletal muscle proliferation and differentiation. Nat Genet 38:228–233
18. Naguibneva I, Ameyar-Zazoua M, Polesskaya A, Ait-Si-Ali S, Groisman R, Souidi M, Cuvellier S, Harel-Bellan A 2006 The microRNA miR-181 targets the homeobox protein Hox-A11 during mammalian myoblast differentiation. Nat Cell Biol 8:278–284
19. Hwang HW, Wentzel EA, Mendell JT 2007 A hexanucleotide element directs microRNA nuclear import. Science 315:97–100
20. Ross SA, Chen X, Hope HR, Sun S, McMahon EG, Broschat K, Gulve EA 2000 Development and comparison of two 3T3-L1 adipocyte models of insulin resistance: increased glucose flux vs glucosamine treatment. Biochem Biophys Res Commun 273:1033–1041
21. Thomson MJ, Williams MG, Frost SC 1997 Development of insulin resistance in 3T3-L1 adipocytes. J Biol Chem 272:7759–7764
22. Buren J, Liu HX, Lauritz J, Eriksson JW 2003 High glucose and insulin in combination cause insulin receptor substrate-1 and -2 depletion and protein kinase B desensitisation in primary cultured rat adipocytes: possible implications for insulin resistance in type 2 diabetes. Eur J Endocrinol 148:157–167
23. Zierath JR, Krook A, Wallberg-Henriksson H 1998 Insulin action in skeletal muscle from patients with NIDDM. Mol Cell Biochem 182:153–160
24. van Dam EM, Govers R, James DE 2005 Akt activation is required at a late stage of insulin-induced GLUT4 translocation to the plasma membrane. Mol Endocrinol 19: 1067–1077
25. Kotani K, Carozzi AJ, Sakaue H, Hara K, Robinson LJ, Clark SF, Yonezawa K, James DE, Kasuga M 1995 Requirement for phosphoinositide 3-kinase in insulin-stim-

ulated GLUT4 translocation in 3T3-L1 adipocytes. Biochem Biophys Res Commun 209:343–348
26. Krek A, Grun D, Poy MN, Wolf R, Rosenberg L, Epstein EJ, MacMenamin P, da Piedade I, Gunsalus KC, Stoffel M, Rajewsky N 2005 Combinatorial microRNA target predictions. Nat Genet 37:495–500
27. John B, Enright AJ, Aravin A, Tuschl T, Sander C, Marks DS 2004 Human microRNA targets. PLoS Biol 2:e363
28. Lewis BP, Burge CB, Bartel DP 2005 Conserved seed pairing, often flanked by adenosines, indicates that thousands of human genes are microRNA targets. Cell 120: 15–20
29. Lewis BP, Shih IH, Jones-Rhoades MW, Bartel DP, Burge CB 2003 Prediction of mammalian microRNA targets. Cell 115:787–798
30. Adams CM, Reitz J, De Brabander JK, Feramisco JD, Li L, Brown MS, Goldstein JL 2004 Cholesterol and 25-hydroxycholesterol inhibit activation of SREBPs by different mechanisms, both involving SCAP and Insigs. J Biol Chem 279:52772–52780
31. Attie AD 2004 Insig: a significant integrator of nutrient and hormonal signals. J Clin Invest 113:1112–1114
32. Engelking LJ, Kuriyama H, Hammer RE, Horton JD, Brown MS, Goldstein JL, Liang G 2004 Overexpression of Insig-1 in the livers of transgenic mice inhibits SREBP processing and reduces insulin-stimulated lipogenesis. J Clin Invest 113:1168–1175
33. Lopez IP, Milagro FI, Marti A, Moreno-Aliaga MJ, Martinez JA, De Miguel C 2004 Gene expression changes in rat white adipose tissue after a high-fat diet determined by differential display. Biochem Biophys Res Commun 318:234–239
34. Kim S, Pak Y 2005 Caveolin-2 regulation of the cell cycle in response to insulin in Hirc-B fibroblast cells. Biochem Biophys Res Commun 330:88–96
35. Macaulay SL, Grusovin J, Stoichevska V, Ryan JM, Castelli LA, Ward CW 2002 Cellular munc18c levels can modulate glucose transport rate and GLUT4 translocation in 3T3L1 cells. FEBS Lett 528:154–160
36. Dulubova I, Sugita S, Hill S, Hosaka M, Fernandez I, Sudhof TC, Rizo J 1999 A conformational switch in syntaxin during exocytosis: role of munc18. EMBO J 18: 4372–4382
37. Vikman J, Ma X, Hockerman GH, Rorsman P, Eliasson L 2006 Antibody inhibition of synaptosomal protein of 25 kDa (SNAP-25) and syntaxin 1 reduces rapid exocytosis in insulin-secreting cells. J Mol Endocrinol 36:503–515
38. Marshall C, Hitman GA, Cassell PG, Turner MD 2007 Effect of glucolipotoxicity and rosiglitazone upon insulin secretion. Biochem Biophys Res Commun 356:756–762
39. Bryant NJ, Govers R, James DE 2002 Regulated transport of the glucose transporter GLUT4. Nat Rev Mol Cell Biol 3:267–277
40. Pekarsky Y, Santanam U, Cimmino A, Palamarchuk A, Efanov A, Maximov V, Volinia S, Alder H, Liu CG, Rassenti L, Calin GA, Hagan JP, Kipps T, Croce CM 2006 Tcl1 expression in chronic lymphocytic leukemia is regulated by miR-29 and miR-181. Cancer Res 66: 11590–11593
41. Noguchi M, Ropars V, Roumestand C, Suizu F 2007 Proto-oncogene TCL1: more than just as a coactivator for Akt. FASEB J 21:2273–2284
42. Cao X, Pfaff SL, Gage FH 2007 A functional study of miR-124 in the developing neural tube. Genes Dev 21: 531–536
43. Hornstein E, Shomron N 2006 Canalization of development by microRNAs. Nat Genet 38(Suppl):S20–S24
44. Lim LP, Lau NC, Garrett-Engele P, Grimson A, Schelter JM, Castle J, Bartel DP, Linsley PS, Johnson JM 2005 Microarray analysis shows that some microRNAs downregulate large numbers of target mRNAs. Nature 433: 769–773
45. Ambros V, Lee RC, Lavanway A, Williams PT, Jewell D 2003 MicroRNAs and other tiny endogenous RNAs in *C. elegans*. Curr Biol 13:807–818
46. Guilherme A, Czech MP 1998 Stimulation of IRS-1-associated phosphatidylinositol 3-kinase and Akt/protein kinase B but not glucose transport by β1-integrin signaling in rat adipocytes. J Biol Chem 273:33119–33122
47. Thurmond DC, Pessin JE 2000 Discrimination of GLUT4 vesicle trafficking from fusion using a temperature-sensitive Munc18c mutant. EMBO J 19:3565–3575

Molecular Endocrinology **is published monthly by The Endocrine Society (http://www.endo-society.org), the foremost professional society serving the endocrine community.**